



## Synthesis and evaluation of sulfonyl piperazine LpxH inhibitors

Seung-Hwa Kwak<sup>a,1</sup>, C. Skyler Cochrane<sup>a,1</sup>, Amanda F. Ennis<sup>a</sup>, Won Young Lim<sup>a</sup>,  
Caroline G. Webster<sup>a</sup>, Jae Cho<sup>b</sup>, Benjamin A. Fenton<sup>b</sup>, Pei Zhou<sup>a,b,\*</sup>, Jiyong Hong<sup>a,c,\*</sup>

<sup>a</sup> Department of Chemistry, Duke University, Durham, NC 27708, United States

<sup>b</sup> Department of Biochemistry, Duke University Medical Center, Durham, NC 27710, United States

<sup>c</sup> Department of Pharmacology and Cancer Biology, Duke University Medical Center, Durham, NC, 27710, United States

### ARTICLE INFO

#### Keywords:

Antibiotics  
Gram-negative bacteria  
Lipid A  
LpxH  
Sulfonyl piperazine  
Structure–activity relationship

### ABSTRACT

The UDP-2,3-diacetylglucosamine pyrophosphate hydrolase LpxH is essential in lipid A biosynthesis and has emerged as a promising target for the development of novel antibiotics against multidrug-resistant Gram-negative pathogens. Recently, we reported the crystal structure of *Klebsiella pneumoniae* LpxH in complex with **1** (AZ1), a sulfonyl piperazine LpxH inhibitor. The analysis of the LpxH-AZ1 co-crystal structure and ligand dynamics led to the design of **2** (JH-LPH-28) and **3** (JH-LPH-33) with enhanced LpxH inhibition. In order to harness our recent findings, we prepared and evaluated a series of sulfonyl piperazine analogs with modifications in the phenyl and *N*-acetyl groups of **3**. Herein, we describe the synthesis and structure–activity relationship of sulfonyl piperazine LpxH inhibitors. We also report the structural analysis of an extended *N*-acyl chain analog **27b** (JH-LPH-41) in complex with *K. pneumoniae* LpxH, revealing that **27b** reaches an untapped polar pocket near the dimanganese cluster in the active site of *K. pneumoniae* LpxH. We expect that our findings will provide designing principles for new LpxH inhibitors and establish important frameworks for the future development of antibiotics against multidrug-resistant Gram-negative pathogens.

### 1. Introduction

Nosocomial infection by multidrug-resistant Gram-negative pathogens is one of the greatest global health challenges [1,2]. However, the lack of financial return on investment has resulted in pharmaceutical companies dropping out from the antibacterial field. As a consequence, no new class of antibiotics for treating Gram-negative bacteria has been approved since the 1980s [1]. At the same time, widespread antibiotic resistance has emerged as a major threat to global health. In light of these issues, the Emerging Infections Network and the WHO cited the lack of both treatment options for Gram-negative bacteria and development pipelines to be the greatest areas of unmet need [1,2]. Therefore, an urgent need exists for a fundamentally new class of antimicrobial therapeutics against Gram-negative pathogens, for which there is no established resistance mechanism.

Gram-negative bacteria are characterized by the presence of a unique cell wall component known as lipopolysaccharide (LPS) or lipooligosaccharide (LOS) in the bacterial outer membrane. Lipid A, a glucosamine-based phospholipid, is the hydrophobic anchor of LPS/LOS.

Lipid A is also an active component of the bacterial endotoxin responsible for Gram-negative septic shock during bacterial infection. As constitutive biosynthesis of lipid A is required for bacterial viability and fitness in the human host [3–5], essential lipid A enzymes are excellent novel antibiotic targets.

Among the nine enzymes involved in lipid A biosynthesis, three functional orthologs (LpxH in  $\beta$ - and  $\gamma$ -proteobacteria [6], LpxI in  $\alpha$ -proteobacteria [7], and LpxG in *Chlamydiae* [8]) carry out the cleavage of the pyrophosphate group of UDP-2,3-diacetylglucosamine (UDP-DAGn) to form lipid X, but they never co-exist. LpxH and LpxG are unique members of the metal-dependent calcineurin-like phosphoesterase (CLP) family, though they share limited sequence similarity [8]; LpxI, on the other hand, is structurally and mechanistically unrelated to LpxH and LpxG [9,10]. Among these three enzymes, LpxH is most widespread, functioning in the vast majority of WHO priority Gram-negative pathogens, including *Pseudomonas aeruginosa*, *Acinetobacter baumannii*, *Klebsiella pneumoniae*, *Escherichia coli*, *Haemophilus influenzae*, and *Neisseria gonorrhoeae*. Therefore, LpxH inhibitors are ideally positioned to overcome this emerging public health crisis.

\* Corresponding authors at: Department of Chemistry, Duke University, Durham, NC 27708, United States and Department of Biochemistry, Duke University Medical Center, Durham, NC 27710, United States.

E-mail addresses: [peizhou@biochem.duke.edu](mailto:peizhou@biochem.duke.edu) (P. Zhou), [jiyong.hong@duke.edu](mailto:jiyong.hong@duke.edu) (J. Hong).

<sup>1</sup> S.-H.K. and C.S.C. contributed equally to this work.

<https://doi.org/10.1016/j.bioorg.2020.104055>

Received 19 May 2020; Received in revised form 8 June 2020; Accepted 26 June 2020

Available online 30 June 2020

0045-2068/ © 2020 Elsevier Inc. All rights reserved.

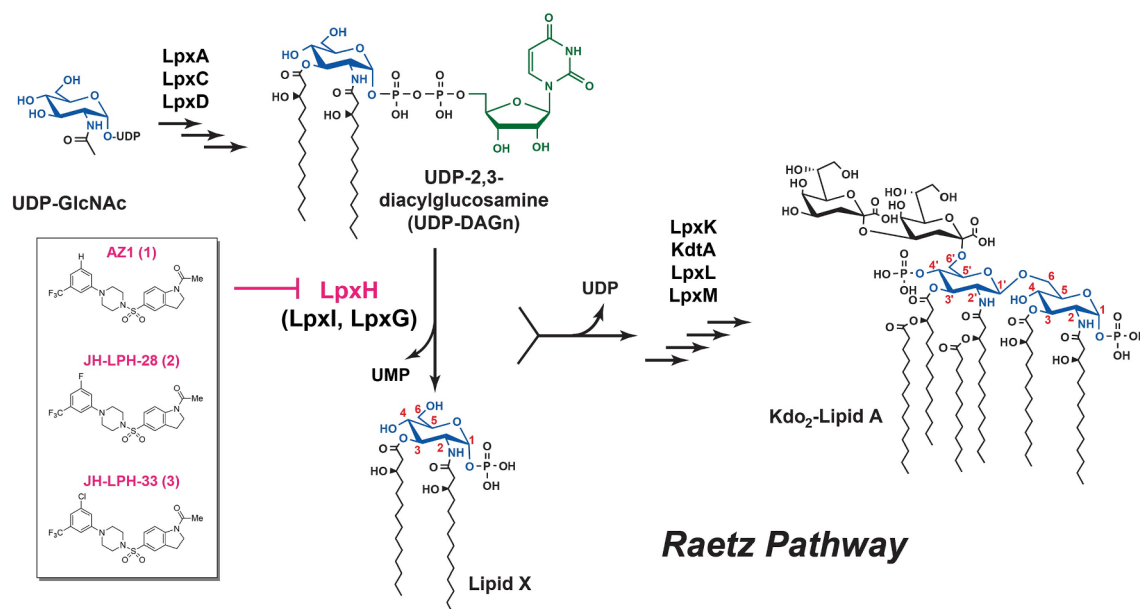


Fig. 1. Sulfonyl piperazine antibiotics inhibit LpxH of the Raetz pathway of lipid A biosynthesis.

A small molecule LpxH inhibitor with a sulfonyl piperazine scaffold (referred to as AZ1 below; chemical structure shown in Fig. 1) was discovered to display antibiotic activity against efflux-deficient *E. coli* strains [11]. We prepared and biochemically evaluated a series of sulfonyl piperazine analogs, and our biochemical characterization established a preliminary structure–activity relationship (SAR) and identified the pharmacophore of this series of LpxH inhibitors [12]. Building upon this work, we recently reported the first crystal structure of *K. pneumoniae* LpxH in complex with AZ1 (1) [13]. We showed that AZ1 fits into the L-shaped acyl chain-binding chamber of LpxH with its indoline ring situated adjacent to the active site, its sulfonyl group adopting a sharp kink, and its *N*-CF<sub>3</sub>-phenyl substituted piperazine group reaching out to the far side of the LpxH acyl chain-binding chamber. The discovery of two <sup>19</sup>F signals of the LpxH-bound AZ1 led us to propose a model of CF<sub>3</sub>-phenyl flipping, which resulted in the design of AZ1 derivatives with the phenyl ring doubly substituted with CF<sub>3</sub> and chloro groups, such as JH-LPH-28 and JH-LPH-33 (2 and 3, respectively; chemical structures shown in Fig. 1) with enhanced potency in enzymatic assays [13]. These designed compounds displayed striking improvement in antibiotic activity over AZ1 against wild-type *K. pneumoniae*, and co-administration with outer membrane permeability enhancers significantly sensitizes *E. coli* to designed LpxH inhibitors.

Encouraged by the promising antibacterial activity of 3, we set off to further explore the SAR of 3. Herein, we describe our efforts toward the synthesis and SAR study of second-generation sulfonyl piperazine analogs with modifications in the head and tail regions in order to further enhance the antibacterial activity of 3. We also report an LpxH inhibitor that occupies a polar binding pocket of *K. pneumoniae* LpxH, which has never been exploited before.

## 2. Results and discussion

### 2.1. Chemistry

AZ1 (1) and JH-LPH-33 (3) consist of three parts (Fig. 1): the substituted phenyl group, sulfonyl piperazine linker, and *N*-acetyl indoline group. Following our previous report that the replacement of the *m*-hydrogen of the phenyl group of 1 with a *m*-chloro substituent significantly enhanced the LpxH inhibition and antibacterial activity of 1 [13], we set out to systematically derivatize the substituents of the phenyl group in order to identify the optimal substituent pattern for

LpxH inhibition. We also envisioned that an extended *N*-acyl chain of 1 and 3 may reach the di-manganese metal cluster in the active site of LpxH, leading to LpxH inhibitors with improved potency. We anticipated that our effort would help the understanding of the effect of various substituents on LpxH inhibition. Such information will allow structural modifications to increase potency and specificity and improve drug performance.

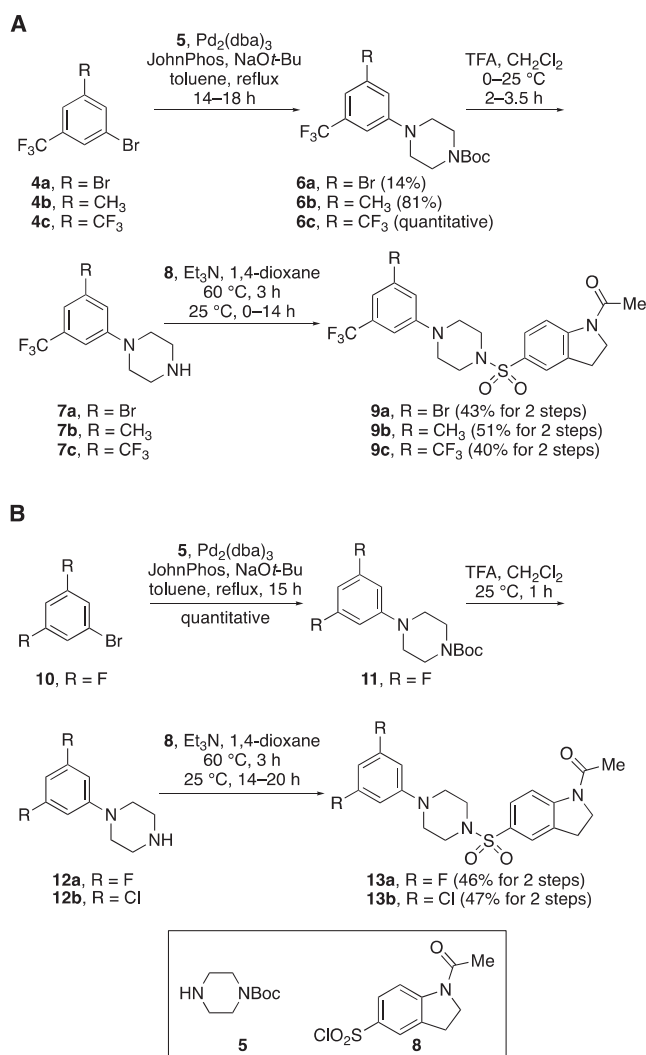
#### 2.1.1. Analogs with aryl group modifications

To gain insights into the importance of the *m*-chloro group of 3 in LpxH inhibition and to evaluate the effect of the size at *m*-position of the phenyl ring of 3, we prepared aryl group analogs by replacing the *m*-chloro group of 3 with various functional groups, including Br, CH<sub>3</sub>, and CF<sub>3</sub> (Scheme 1). Our previous synthesis of 3 [13] provided the basis for the synthesis of *m*-bromo analog 9a, *m*-methyl analog 9b, and *m*-trifluoromethyl analog 9c (Scheme 1A). Starting from commercially available 1,3-dibromo-5-(trifluoromethyl)benzene (4a), Pd-mediated coupling of 4a with 1-Boc-piperazine (5) provided the Boc-protected *N*-aryl piperazine 6a. Boc deprotection of 6a by treatment with TFA followed by coupling of the resulting piperazine 7a with commercially available 1-acetyl-5-indolinesulfonyl chloride (8) in the presence of Et<sub>3</sub>N proceeded smoothly to afford the desired *m*-bromo analog 9a in 43% for 2 steps. The *m*-methyl analog 9b and the *m*-trifluoromethyl analog 9c were also prepared in a similar manner starting from the commercially available 1-bromo-3-methyl-5-(trifluoromethyl)benzene (4b) and 1,3-bis(trifluoromethyl)-5-bromobenzene (4c), respectively.

To evaluate the effect of symmetrical substituents, we prepared the *m*-difluoro analog 13a and the *m*-dichloro analog 13b (Scheme 1B). Commercially available 1-bromo-3,5-difluorobenzene (10) was coupled to 1-Boc-piperazine (5) to afford the *N*-aryl piperazine 11. Boc deprotection of 11 followed by coupling of the resulting piperazine 12a to 1-acetyl-5-indolinesulfonyl chloride (8) completed the synthesis of the *m*-difluoro analog 13a. Similarly, the *m*-dichloro analog 13b was prepared by coupling commercially available 1-(3,5-dichlorophenyl)piperazine (12b) with 8.

#### 2.1.2. Analogs with indoline modifications

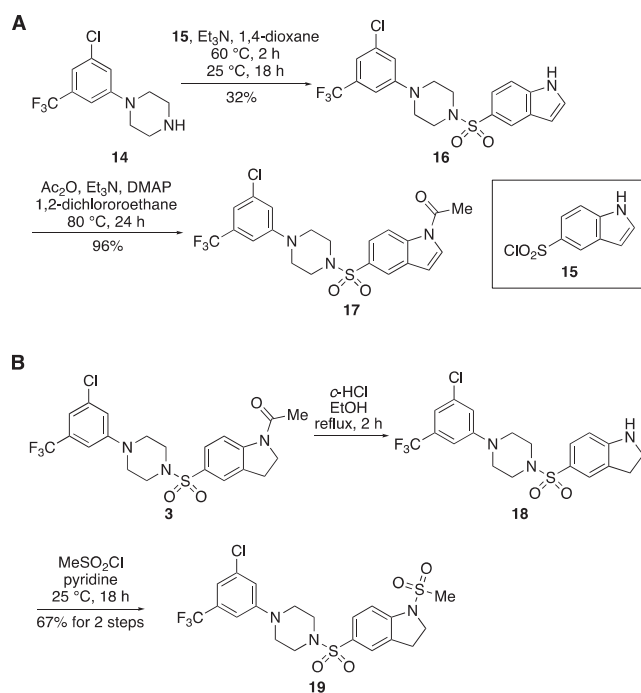
We also synthesized an indole analog 17 and an *N*-methanesulfonyl group analog 19 by replacing the indoline and *N*-acetyl group of 3 with an indole group and a methanesulfonyl group, respectively. 1-(3-Chloro-5-(trifluoromethyl)phenyl)piperazine (14) [13] was coupled to



1H-indole-5-sulfonyl chloride (**15**) to give **16** (Scheme 2A). *N*-Acetylation of the indole ring of **16** by treatment with Ac<sub>2</sub>O completed the synthesis of the indole analog **17**. Compound **3** was converted to the *N*-methanesulfonyl group analog **19** by Ac deprotection under acidic conditions followed by *N*-methanesulfonylation of the resulting indoline.

### 2.1.3. Analogs with extended *N*-acyl chains

In order to explore the role of the *N*-acetyl group of **3** in LpxH inhibition, we prepared several sulfonyl piperazine compounds with extended *N*-acyl chains. Since LpxH contains two manganese metals in the active site, we hypothesized that a sulfonyl piperazine LpxH inhibitor that exploits the chelation to the di-manganese metal cluster would be more potent than the parent compounds, **1** or **3**. Therefore, we capped the *N*-acyl group with a hydroxamic acid since hydroxamic acid is a well-characterized manganese-chelating group [14]. We envisioned the hydroxamic acid group would tightly bind to the manganese metals in the LpxH active site and improve the binding affinity of LpxH inhibitors. Since the *N*-acetylsulfanilyl analog of **1** was active in our previous study [12], we modeled our new extended *N*-acyl chain analogs based on a sulfanilamide scaffold. Starting from the known 4-((4-(3-(trifluoromethyl)phenyl)piperazin-1-yl)sulfonyl)aniline (**20a**) [12], we successfully introduced a urea linkage with methyl 4-aminobutanoate in the presence of CDI (Scheme 3A). To install a hydroxamic acid group, we hydrolyzed the methyl ester **21** to the corresponding



carboxylic acid **22** and then coupled **22** with NH<sub>2</sub>OTBS. The final TBS deprotection of **23** by TFA successfully afforded the extended *N*-acyl chain hydroxamic acid analog **24**. To gain insights into the effect of chain length on LpxH inhibition, we further elongated the acyl chain by replacing methyl 4-aminobutanoate with methyl 5-aminopentanoate and prepared the analogs **27a** and **27b** (Scheme 3B).

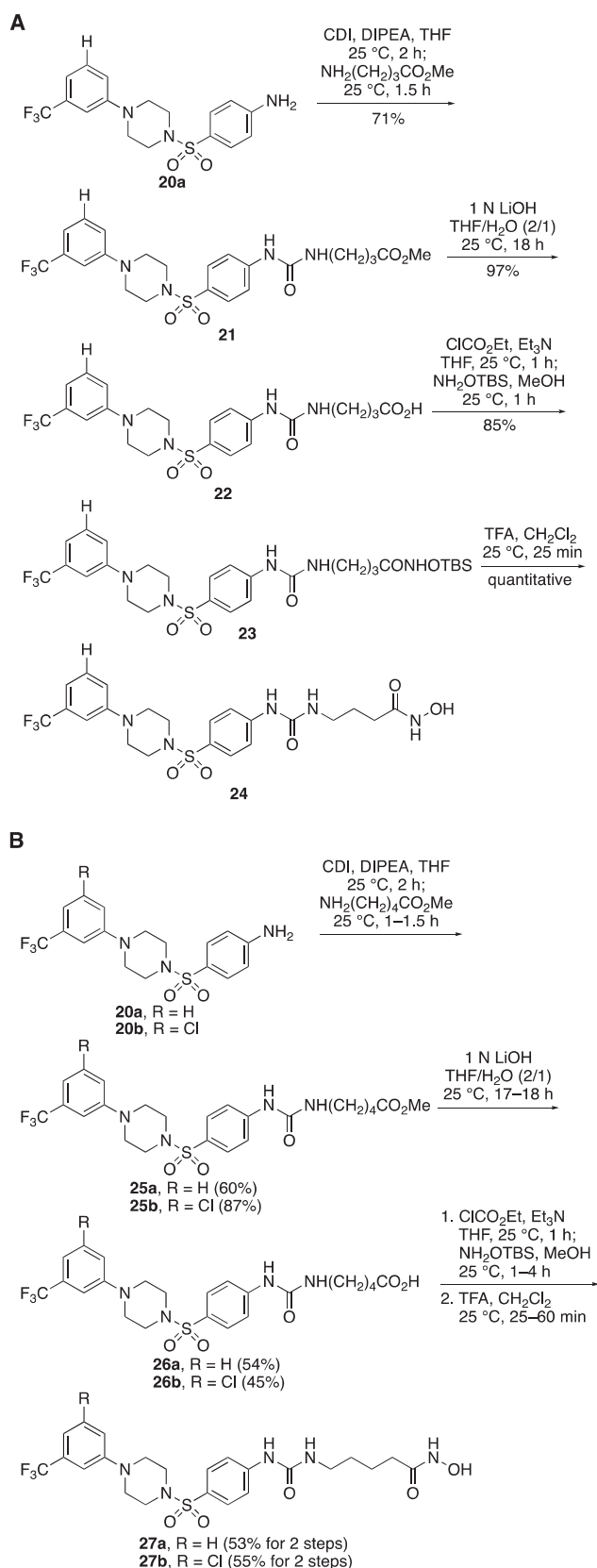
## 2.2. Analysis of structure–activity relationships

### 2.2.1. Substituted phenyl and indoline analogs

After the completion of analog synthesis, we biochemically characterized the *K. pneumoniae* LpxH inhibition by these analogs at 0.1 μM using the nonradioactive, colorimetric malachite green assay that we had previously reported [12]. Among the tested analogs, nearly all of the compounds show comparable or better activity than **1** (AZ1, 22% inhibition; Table 1). The extended *N*-acyl chain analog **27b** (JH-LPH-41) showed the strongest inhibition of LpxH activity and inhibited ~64% of LpxH activity. Such an activity is only slightly worse than **3** (JH-LPH-33, 79% inhibition), but it is better than **2** (JH-LPH-28, 48% inhibition). Several other analogs, including **9a** (57% inhibition), **9b** (50% inhibition), **13b** (59% inhibition), and **17** (48% inhibition), also showed noticeable LpxH inhibition, whereas **9c** (16% inhibition), **19** (12% inhibition), and **24** (15% inhibition) showed significantly lower activity than **3**, but their activities were comparable to **1** (Table 1).

The LpxH activity assay data provided several valuable insights into the SAR of sulfonyl piperazine LpxH inhibitors (Fig. 2). Among the phenyl group analogs of **3** with a second *m*-substituent of the *m*-trifluoromethyl substituted phenyl ring (e.g., *m*-hydrogen substituted analog **1**, *m*-fluoro substituted analog **2**, *m*-methyl substituted analog **9b**, and *m*-chloro substituted analog **3**), there is a general trend of increasing potency following the increase in the volume of substituents (H < F < CH<sub>3</sub> < Cl), except for *m*-bromo substituted analog **9a** and *m*-trifluoromethyl substituted analog **9c**, which may have become too bulky for the buried acyl chain chamber to tolerate [13].

A similar trend was also observed when both *m*-positions are substituted with fluoro (analog **13a**), chloro (analog **13b**), and trifluoromethyl (analog **9c**) groups, with the dichloro substituted analog **13b** displaying better activity (59% inhibition) than the difluoro



Scheme 3. Synthesis of analogs with extended acyl chains.

substituted analog **13a** (39% inhibition) and the difluoromethyl substituted analog **9c** (16% inhibition).

Replacement of the indoline of **3** with indole (analog **17**) slightly decreased the potency (48% inhibition for **17** vs 79% inhibition for **3**).

When the *N*-acetyl group of the indoline ring of **3** was replaced with a methanesulfonyl group (analog **19**), the activity dropped significantly (12% inhibition), indicating that the *N*-acetyl group of **3** is critical to the LpxH inhibition.

### 2.2.2. Extended *N*-acyl chain analogs

As our previous structural analysis of LpxH in complex with **1** and **3** has shown that the active site of LpxH was not occupied by sulfonyl piperazine LpxH inhibitors such as **1** or **3** [13], we synthesized analogs with extended acyl chains to test the feasibility of expanding the compound-LpxH interaction to the active site. For proof-of-concept studies, we selected the sulfanilamide scaffold and attached an extended acyl chain to the aniline nitrogen. Three compounds (**24**, **27a**, and **27b**) were synthesized containing different lengths of acyl chains with a terminal hydroxamate group designed to chelate the di-manganese cluster in the active site. The shorter *N*-acyl chain analog **24** showed slightly lower activity (15% inhibition) than **1** (22% inhibition), whereas extending the acyl chain of **24** by one methylene group (analog **27a**, 30% inhibition) improved the potency over **1**. Considering that aryl replacement of the indoline ring always results in reduced activity [12], attaching an acyl chain generally improves the potency of the compound. Combining the long acyl chain with the phenyl ring doubly substituted with trifluoromethyl and chloro groups yielded the most active compound of this series **27b** (JH-LPH-41) that inhibited 64% activity of KpLpxH at 0.1 μM compound concentration. The activity of **27b** is only slightly worse than **3** (79% inhibition). Despite the excellent *in vitro* activity of **27b**, its long acyl chain with many rotatable bonds negatively impacted the antibiotic activity of **27b**, yielding an unimpressive MIC of 32 μg/mL against *K. pneumoniae*. The MIC value **27b** was still an improvement over **1** (MIC > 64 μg/mL), but is significantly worse than **3** (1.6 μg/mL) [13]. Such a result was attributed to the poor membrane permeability of **27b** due to the highly flexible and hydrophobic nature of the extended acyl chain of **27b**.

### 2.3. Structure of *K. pneumoniae* LpxH in complex with **27b** (JH-LPH-41)

In order to gain a better understanding of the nature of the interaction of **27b** with *K. pneumoniae* LpxH, we determined the co-crystal structure of the *K. pneumoniae* LpxH/**27b** complex at 1.85 Å (Fig. 3, Figure S1, and Table S1). We found that, similar to previously reported sulfonyl piperazine compound structures, [13] **27b** also occupies the hydrophobic substrate-binding chamber between the calcineurin-like phosphatase (CLP) domain and the insertion cap domain (Fig. 3A). However, its *N*-acyl chain snakes into the active site as designed: the acyl chain picks up additional hydrophobic interactions with Y125 of the insertion cap and I171 on the loop connecting the cap back to the CLP core domain (Fig. 3B). Most unexpectedly, the hydroxamate group did not chelate the di-manganese cluster as we designed; instead, its carbonyl group and *N*-hydroxyl group form two hydrogen bonds with the backbone amide and carbonyl group of M172 of the same loop as I171 (Fig. 3B). Although these hydroxamate-containing acyl chains did not reach the metal cluster as we designed, they demonstrate the feasibility to expand molecular interactions into the active site of LpxH.

## 3. Conclusion

We recently reported the first crystal structure of *K. pneumoniae* LpxH in complex with AZ1 (**1**), a sulfonyl piperazine LpxH inhibitor, and the identification of a more potent LpxH inhibitor, JH-LPH-33 (**3**). In order to further elaborate the SAR of these compounds, we prepared and biochemically characterized a series of sulfonyl piperazine LpxH inhibitors. Our SAR study revealed an important correlation between the compound activity and the volume of the functional groups at the *meta*-position of the trifluoromethyl substituted distal phenyl ring, with the compound potency increasing from H, F, CH<sub>3</sub> and achieving maximal activity at Cl substitution. Further increases in volume with Br and

**Table 1**  
Specific activity *K. pneumoniae* LpxH in the presence of sulfonyl piperazine LpxH inhibitors.

| Compounds       | Structure | 0.1 $\mu\text{M}$ compound Activity ( $\mu\text{mol}/\text{min}/\text{mg}$ ) <sup>a</sup> | Percentage Activity | Percentage Inhibition |
|-----------------|-----------|---|---------------------|-----------------------|
| DMSO            |           | 298.7 $\pm$ 9.0   | 100 $\pm$ 3         | 0                     |
| 1 (AZ1)         |           |   | 78 <sup>b</sup>     | 22                    |
| 2 (JH-LPH-28)   |           |   | 52 <sup>b</sup>     | 48                    |
| 3 (JH-LPH-33)   |           |   | 21 <sup>b</sup>     | 79                    |
| 9a              |           | 128.3 $\pm$ 12  | 43 $\pm$ 4          | 57                    |
| 9b              |           | 148.8 $\pm$ 9.3   | 50 $\pm$ 3          | 50                    |
| 9c              |           | 252.1 $\pm$ 38.9  | 84 $\pm$ 13         | 16                    |
| 13a             |           | 182.4 $\pm$ 16.7  | 61 $\pm$ 6          | 39                    |
| 13b             |           | 121.7 $\pm$ 25.1  | 41 $\pm$ 8          | 59                    |
| 17              |           | 156.1 $\pm$ 15.2  | 52 $\pm$ 5          | 48                    |
| 19              |           | 262.7 $\pm$ 34.7  | 88 $\pm$ 12         | 12                    |
| 24              |           | 253.3 $\pm$ 20.0  | 85 $\pm$ 7          | 15                    |
| 27a             |           | 210.0 $\pm$ 26.3  | 70 $\pm$ 9          | 30                    |
| 27b (JH-LPH-41) |           | 107.6 $\pm$ 15.6  | 36 $\pm$ 5          | 64                    |

<sup>a</sup> Data are mean values of three independent experiments. Errors represent standard error.

<sup>b</sup> Values calculated from previously reported IC<sub>50</sub> curves [13] obtained under identical assay conditions.

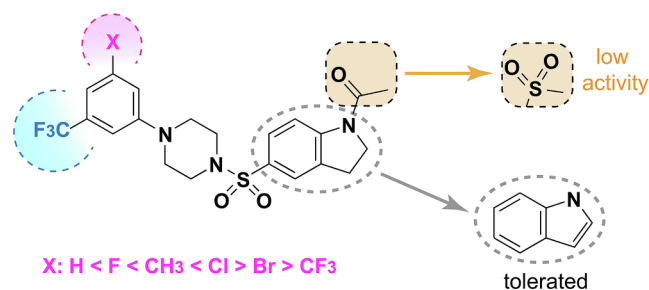


Fig. 2. SAR of phenyl and indoline substitutions.

CF<sub>3</sub> substitutions resulted in reduced activity. A similar trend was observed with the symmetrical substitutions at the *meta*-positions of the distal phenyl ring. Moreover, our efforts resulted in the identification of **27b** (JH-LPH-41) that occupies a previously untapped pocket near the di-manganese cluster in the LpxH active site. Despite having a proximal phenyl group instead of an indoline group, the acyl chain extension of **27b** into the active site nearly restored the *in vitro* activity of **27b** to that of **3** with an indoline group. These findings establish a clear SAR of the *m*-substituted distal phenyl ring and demonstrate the feasibility to expand drug interactions to the active site of LpxH. We anticipate our study will ultimately contribute to developing more potent and selective LpxH inhibitors for multidrug-resistant Gram-negative pathogens.

## 4. Materials and methods

### 4.1. Synthesis of sulfonyl piperazine LpxH inhibitors

**General chemistry procedures.** All reactions were conducted in oven-dried glassware under nitrogen or argon. Unless otherwise stated all reagents were purchased from commercial suppliers and used without further purification. All solvents were American Chemical Society (ACS) grade or better and used without further purification except tetrahydrofuran (THF), which was freshly distilled from sodium/benzophenone each time before use. Analytical thin layer chromatography (TLC) was performed with glass backed silica gel (60 Å) plates with fluorescent indication (Whatman). Visualization was accomplished by UV irradiation at 254 nm and/or by staining with *p*-anisaldehyde solution. Flash column chromatography was performed by using silica gel (particle size 230–400 mesh, 60 Å). All <sup>1</sup>H NMR spectra were recorded with a Varian 400 spectrometer. All <sup>1</sup>H NMR  $\delta$  values are given in parts per million (ppm) and are referenced to the residual solvent signals (CDCl<sub>3</sub>:  $\delta$  = 7.26 ppm, CD<sub>3</sub>OD:  $\delta$  = 3.31 ppm, CD<sub>3</sub>COCD<sub>3</sub>:  $\delta$  = 2.05 ppm). Coupling constants (*J*) are given in Hertz (Hz) and multiplicities are indicated using the conventional abbreviation (s = singlet, d = doublet, t = triplet, q = quartet, m = multiplet or overlap of non-

equivalent resonances, br = broad). Electrospray ionization (ESI) mass spectrometry (MS) was recorded with an Agilent 1100 series (LC/MSD trap) spectrometer in order to obtain the molecular masses of compounds. The purity of final compounds used in bioassays was determined by NMR and was found to be > 95%.

*tert*-Butyl 4-(3-bromo-5-(trifluoromethyl)phenyl)piperazine-1-carboxylate (**6a**). Anhydrous toluene (4.8 mL) was added to a mixture of 1,3-dibromo-5-(trifluoromethyl)benzene (**4a**, 500 mg, 1.6 mmol), 1-Boc-piperazine (**5**, 596 mg, 3.2 mmol), NaOt-Bu (307 mg, 3.2 mmol), JohnPhos (71.6 mg, 0.24 mmol), and Pd<sub>2</sub>(dba)<sub>3</sub> (68.6 mg, 0.08 mmol). Argon (Ar) was bubbled through the reaction mixture for 15 min before the reaction mixture was heated to reflux for 14 h. The reaction mixture was concentrated *in vacuo*, dissolved in CH<sub>2</sub>Cl<sub>2</sub>/MeOH (1/1), and filtered through a pad of Celite. The filtrate was concentrated *in vacuo* and purified by column chromatography (silica gel, hexanes/EtOAc, 5/1) to afford **6a** (100 mg, 14%) as a yellow solid: <sup>1</sup>H NMR (400 MHz, CDCl<sub>3</sub>)  $\delta$  7.20 (s, 1H), 7.15 (s, 1H), 7.01 (s, 1H), 3.61–3.53 (m, 4H), 3.23–3.15 (m, 4H), 1.48 (s, 9H); HRMS (ESI) *m/z* 431.0545 [(M + Na)<sup>+</sup> calcd for C<sub>16</sub>H<sub>20</sub>BrF<sub>3</sub>N<sub>2</sub>O<sub>2</sub> 431.0553].

1-(3-Bromo-5-(trifluoromethyl)phenyl)piperazine (**7a**). To a cooled (0 °C) solution of **6a** (100 mg, 0.22 mmol) in anhydrous CH<sub>2</sub>Cl<sub>2</sub> (1 mL) was added dropwise TFA (0.5 mL). After stirring at 25 °C for 2.5 h, the solvents were removed under reduced pressure to give **7a** (100 mg) as an orange solid. Compound **7a** was used in the following step without further purification: <sup>1</sup>H NMR (400 MHz, CDCl<sub>3</sub>)  $\delta$  9.35 (br s, 1H), 7.34 (s, 1H), 7.21 (s, 1H), 7.05 (s, 1H), 3.50 (t, *J* = 5.1 Hz, 4H), 3.45–3.36 (m, 4H); HRMS (ESI) *m/z* 309.0216 [(M + H)<sup>+</sup> calcd for C<sub>11</sub>H<sub>12</sub>BrF<sub>3</sub>N<sub>2</sub> 309.0209].

1-(5-((4-(3-Bromo-5-(trifluoromethyl)phenyl)piperazin-1-yl)sulfonyl)indolin-1-yl)ethan-1-one (**9a**). A solution of **7a** (100 mg, 0.32 mmol) and Et<sub>3</sub>N (50  $\mu$ L, 0.38 mmol) in anhydrous 1,4-dioxane (0.22 M, 1.5 mL) was heated to 60 °C. 1-Acetylidoline-5-sulfonyl chloride (**8**, 41.5 mg, 0.16 mmol) in anhydrous 1,4-dioxane (1 mL) was added to the reaction mixture. After stirring at 60 °C for 3 h, the reaction mixture was cooled to 25 °C. The reaction was quenched by an addition of H<sub>2</sub>O and the resulting mixture was extracted with EtOAc. The combined organic layers were washed with brine, dried over anhydrous Na<sub>2</sub>SO<sub>4</sub>, and concentrated *in vacuo*. The residue was purified by column chromatography (silica gel, hexanes/EtOAc, 1/1) to afford **9a** (37 mg, 43% for 2 steps) as a white solid: <sup>1</sup>H NMR (400 MHz, CDCl<sub>3</sub>)  $\delta$  8.34 (d, *J* = 8.5 Hz, 1H), 7.63 (d, *J* = 8.4 Hz, 1H), 7.57 (s, 1H), 7.21 (s, 1H), 7.09 (s, 1H), 6.95 (s, 1H), 4.16 (t, *J* = 8.6 Hz, 2H), 3.34–3.24 (m, 6H), 3.17–3.11 (m, 4H), 2.27 (s, 3H); HRMS (ESI) *m/z* 532.0517 [(M + H)<sup>+</sup> calcd for C<sub>21</sub>H<sub>21</sub>BrF<sub>3</sub>N<sub>3</sub>O<sub>3</sub>S 532.0512].

*tert*-Butyl 4-(3-methyl-5-(trifluoromethyl)phenyl)piperazine-1-carboxylate (**6b**). To a solution of 1-bromo-3-methyl-5-(trifluoromethyl)benzene (**4b**, 50 mg, 0.21 mmol), 1-Boc-piperazine (**5**, 51 mg, 0.27 mmol), and NaOt-Bu (30 mg, 0.31 mmol) in toluene (0.63 mL) was

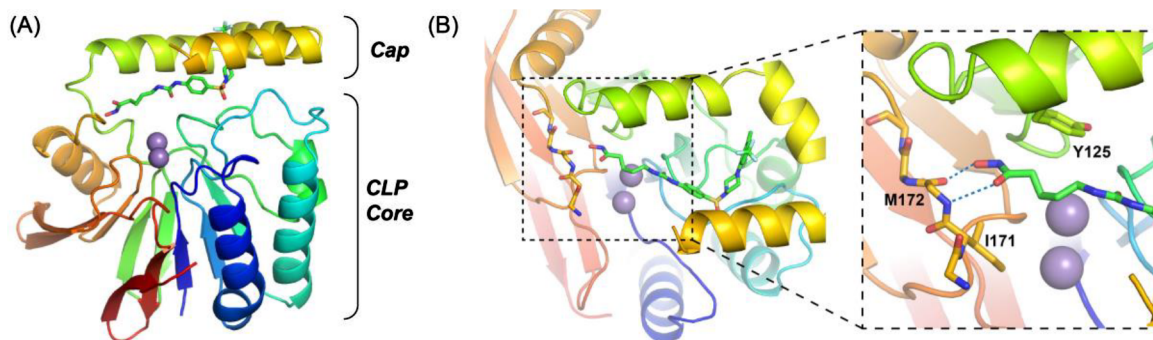


Fig. 3. Expansion of the LpxH inhibitor interaction into the active site of LpxH. (A) Side view of the KpLpxH/**27b** (JH-LPH-41) complex. LpxH is shown in the cartoon model, the catalytic di-manganese cluster is shown in the sphere model, and **27b** is shown in the stick model. Location of the cap domain and the CLP core domain is labeled. (B) Top view of the KpLpxH/**27b** complex. Hydrophobic residues of LpxH (Y125 and I171) interacting with the *N*-acyl chain of **27b** are labeled. The hydrogen bonds between the hydroxamate group of **27b** and the backbone of M172 of LpxH are indicated by dashed lines.

added JohnPhos (6.3 mg, 0.02 mmol, 10 mol%), and Pd<sub>2</sub>(dba)<sub>3</sub> (9.2 mg, 0.01 mmol, 5 mol%). Argon (Ar) was bubbled through the reaction mixture for 15 min and then the reaction was heated to reflux for 15 h. The reaction mixture was concentrated *in vacuo*, dissolved in CH<sub>2</sub>Cl<sub>2</sub>/MeOH (1/1), and filtered through a pad of Celite. The residue was purified by column chromatography (silica gel, hexanes/EtOAc, 20/1) to afford **6b** (58 mg, 81%): <sup>1</sup>H NMR (400 MHz, CDCl<sub>3</sub>) δ 6.92 (s, 2H), 6.87 (s, 1H), 3.62–3.51 (m, 4H), 3.21–3.08 (m, 4H), 2.35 (s, 3H), 1.47 (s, 9H).

1-(3-Methyl-5-(trifluoromethyl)phenyl)piperazine (**7b**). To a solution of **6b** (58 mg, 0.17 mmol) in CH<sub>2</sub>Cl<sub>2</sub> (0.85 mL) was added TFA (0.33 mL). The reaction mixture was stirred at 25 °C for 2 h and then was concentrated *in vacuo* to afford **7b** (41 mg). Compound **7b** was used in the following step without further purification: <sup>1</sup>H NMR (400 MHz, CDCl<sub>3</sub>) δ 7.03 (s, 1H), 6.93 (s, 1H), 6.88 (s, 1H), 3.60–3.46 (m, 4H), 2.58–2.40 (m, 4H), 2.37 (s, 3H).

1-(5-((4-(3-Methyl-5-(trifluoromethyl)phenyl)piperazin-1-yl)sulfonyl)indolin-1-yl)ethan-1-one (**9b**). A solution of **7b** (27 mg, 0.11 mmol) and Et<sub>3</sub>N (17 μL, 0.13 mmol) in 1,4-dioxane (1.63 mL) was heated to 60 °C. To this solution, 1-acetylindoline-5-sulfonyl chloride (**8**, 29 mg, 0.11 mmol) was added and the resulting mixture was stirred at 60 °C for 3 h followed by at 25 °C for 14 h. The reaction was quenched by an addition of H<sub>2</sub>O and the aqueous layer was extracted with EtOAc. The combined organic layers were dried over anhydrous Na<sub>2</sub>SO<sub>4</sub> and concentrated *in vacuo*. The crude product was purified by column chromatography (silica gel, hexanes/EtOAc, 2/1) to afford **9b** (26.3 mg, 51% for 2 steps): <sup>1</sup>H NMR (400 MHz, CDCl<sub>3</sub>) δ 8.33 (d, *J* = 7.9 Hz, 1H), 7.62 (d, *J* = 7.9 Hz, 1H), 7.56 (s, 1H), 6.93 (s, 1H), 6.85 (s, 1H), 6.82 (s, 1H), 4.14 (t, *J* = 8.6 Hz, 2H), 3.31–3.22 (m, 6H), 3.18–3.10 (m, 4H), 2.32 (s, 3H), 2.25 (s, 3H); HRMS (ESI) *m/z* 468.1554 [(M + H)<sup>+</sup> calcd for C<sub>22</sub>H<sub>24</sub>F<sub>3</sub>N<sub>3</sub>O<sub>3</sub>S 468.1563].

*tert*-Butyl 4-(3,5-bis(trifluoromethyl)phenyl)piperazine-1-carboxylate (**6c**). Toluene (1.6 mL) was added to a mixture of 1,3-bis(trifluoromethyl)-5-bromobenzene (**4c**, 150 mg, 0.51 mmol), 1-Boc-piperazine (**5**, 123 mg, 0.66 mmol), NaOt-Bu (74 mg, 0.77 mmol), JohnPhos (15 mg, 10 mol%), and Pd<sub>2</sub>(dba)<sub>3</sub> (28 mg, 5 mol%). Argon (Ar) was bubbled through the reaction mixture for 30 min, and the reaction mixture was refluxed for 18 h. The reaction mixture was concentrated *in vacuo* and the residue was dissolved in CH<sub>2</sub>Cl<sub>2</sub>/MeOH (1/1), filtered through a pad of Celite, and concentrated *in vacuo*. The residue was purified by column chromatography (silica gel, hexanes/EtOAc, 20/1) to afford **6c** (203 mg, quantitative): <sup>1</sup>H NMR (400 MHz, CDCl<sub>3</sub>) δ 7.30 (s, 1H), 7.25 (s, 2H), 3.65–3.59 (m, 4H), 3.27–3.24 (m, 4H), 1.48 (s, 9H).

1-(3,5-Bis(trifluoromethyl)phenyl)piperazine (**7c**). To a solution of **6c** (200 mg, 0.5 mmol) in CH<sub>2</sub>Cl<sub>2</sub> (3 mL) was added TFA (1.3 mL) at 0 °C. The reaction mixture was stirred under N<sub>2</sub> at 0 °C for 10 min and then warmed to 25 °C. The reaction mixture was stirred under N<sub>2</sub> at 25 °C for 3.5 h. The reaction mixture was concentrated *in vacuo* to give **7c** as an orange solid. Compound **7c** was used in the following step without further purification: <sup>1</sup>H NMR (400 MHz, CDCl<sub>3</sub>) δ 7.45 (s, 1H), 7.30 (s, 2H), 3.95 (br s, 1H), 3.59 (m, 4H), 3.46 (m, 4H).

1-(5-((4-(3,5-Bis(trifluoromethyl)phenyl)piperazin-1-yl)sulfonyl)indolin-1-yl)ethan-1-one (**9c**). To a solution of **7c** (50 mg, 0.17 mmol) in 1,4-dioxane (3 mL) was added Et<sub>3</sub>N (32 μL, 0.24 mmol) at 25 °C. 1-Acetyl-5-indoline sulfonyl chloride (**8**, 44 mg, 0.17 mmol) was added to the reaction mixture. The resulting mixture was stirred under N<sub>2</sub> at 60 °C for 3 h. The reaction mixture was cooled to 25 °C and kept at the same temperature for 10 h. The reaction mixture was diluted with EtOAc. The layers were separated, and the aqueous layer was extracted with EtOAc. The combined organic layers were washed with brine, dried over anhydrous Na<sub>2</sub>SO<sub>4</sub>, and concentrated under reduced pressure. The residue was purified by column chromatography (silica gel, hexanes/EtOAc, 4/1) to afford **9c** as a white solid (35 mg, 40% for 2 steps): <sup>1</sup>H NMR (400 MHz, CDCl<sub>3</sub>) δ 8.34 (d, *J* = 8.6 Hz, 1H), 7.62 (dd, *J* = 8.5, 1.9 Hz, 1H), 7.57 (s, 1H), 7.31 (s, 1H), 7.19 (s, 2H), 4.17 (t,

*J* = 8.5 Hz, 2H), 3.36–3.34 (m, 4H), 3.28 (t, *J* = 8.8 Hz, 2H), 3.16–3.15 (m, 4H), 2.27 (s, 3H); HRMS (ESI) *m/z* 522.1281 [(M + H)<sup>+</sup> calcd for C<sub>22</sub>H<sub>21</sub>F<sub>6</sub>N<sub>3</sub>O<sub>3</sub>S 522.1289].

*tert*-Butyl 4-(3,5-difluorophenyl)piperazine-1-carboxylate (**11**). Toluene (4 mL) was added to a mixture of 1-bromo-3,5-difluorobenzene (**10**, 250 mg, 1.3 mmol), 1-Boc-piperazine (**5**, 315 mg, 1.69 mmol), NaOt-Bu (187 mg, 1.95 mmol), JohnPhos (39 mg, 10 mol%), and Pd<sub>2</sub>(dba)<sub>3</sub> (60 mg, 5 mol%). Argon (Ar) was bubbled through the reaction mixture for 30 min, and the reaction mixture was refluxed for 15 h. The reaction mixture was concentrated *in vacuo* and the residue was dissolved in CH<sub>2</sub>Cl<sub>2</sub>/MeOH (1/1), filtered through a pad of Celite, and concentrated *in vacuo*. The residue was purified by column chromatography (silica gel, hexanes/EtOAc, 20/1) to afford **11** (436 mg, quantitative) as a solid: <sup>1</sup>H NMR (400 MHz, CDCl<sub>3</sub>) δ 6.36 (d, *J* = 8.8 Hz, 2H), 6.27 (t, *J* = 8.8 Hz, 1H), 3.60–3.52 (m, 4H), 3.20–3.11 (m, 4H), 1.48 (s, 9H).

1-(3,5-Difluorophenyl)piperazine (**12a**). TFA (1.4 mL) was added to a solution of **11** (207 mg, 0.69 mmol) in CH<sub>2</sub>Cl<sub>2</sub> (3.5 mL), and the resulting mixture was stirred at 25 °C for 1 h. The reaction mixture was concentrated *in vacuo* to afford **12a**. Compound **12a** was used in the following step without further purification: <sup>1</sup>H NMR (400 MHz, CD<sub>3</sub>OD) δ 6.61 (d, *J* = 10.0 Hz, 2H), 6.42 (t, *J* = 9.0 Hz, 1H), 3.48–3.45 (m, 4H), 3.36–3.33 (m, 4H); HRMS (ESI) *m/z* 199.1041 [(M + H)<sup>+</sup> calcd for C<sub>10</sub>H<sub>12</sub>F<sub>2</sub>N<sub>2</sub> 199.1041].

1-(5-((4-(3,5-Difluorophenyl)piperazin-1-yl)sulfonyl)indolin-1-yl)ethan-1-one (**13a**). A solution of **12a** (50 mg, 0.25 mmol) and Et<sub>3</sub>N (40 μL, 0.3 mmol) in 1,4-dioxane (3.7 mL) was heated to 60 °C and 1-acetyl-5-indolinesulfonyl chloride (**8**, 65 mg, 0.25 mmol) was added. After stirring at 60 °C for 3 h, the reaction mixture was cooled to 25 °C and stirred for additional 14 h. The reaction was quenched by an addition of H<sub>2</sub>O. The reaction mixture was extracted with EtOAc. The combined organic layers were dried over anhydrous Na<sub>2</sub>SO<sub>4</sub> and concentrated *in vacuo*. The residue was purified by column chromatography (silica gel, hexanes/EtOAc, 1/1) to afford **13a** (48 mg, 46% for 2 steps) as a white solid: <sup>1</sup>H NMR (400 MHz, CDCl<sub>3</sub>) δ 8.34 (d, *J* = 8.2 Hz, 1H), 7.62 (d, *J* = 8.2 Hz, 1H), 7.56 (s, 1H), 6.31–6.25 (m, 3H), 4.16 (t, *J* = 8.5 Hz, 2H), 3.30–3.26 (m, 6H), 3.12–3.11 (m, 4H), 2.26 (s, 3H); HRMS (ESI) *m/z* 422.1349 [(M + H)<sup>+</sup> calcd for C<sub>20</sub>H<sub>21</sub>F<sub>2</sub>N<sub>3</sub>O<sub>3</sub>S 422.1345].

1-(5-((4-(3,5-Dichlorophenyl)piperazin-1-yl)sulfonyl)indolin-1-yl)ethan-1-one (**13b**). To a solution of commercially available 1-(3-(5-dichlorophenyl)piperazine (**12a**, 50 mg, 0.22 mmol) in 1,4-dioxane (3.0 mL) was added Et<sub>3</sub>N (34 μL, 0.26 mmol) at 25 °C. The reaction mixture was treated with 1-acetyl-5-indoline sulfonyl chloride (**8**, 57 mg, 0.22 mmol) and stirred under N<sub>2</sub> at 60 °C for 3 h. The reaction mixture was cooled to 25 °C and then stirred for an additional 20 h. The reaction mixture was diluted with EtOAc. The layers were separated, and the aqueous layer was extracted with EtOAc. The combined organic layers were washed with brine, dried over anhydrous Na<sub>2</sub>SO<sub>4</sub>, and concentrated *in vacuo*. The residue was purified by column chromatography (silica gel, hexanes/EtOAc, 4/1) to afford **13b** as a white solid (46 mg, 47%): <sup>1</sup>H NMR (400 MHz, CDCl<sub>3</sub>) δ 8.34 (d, *J* = 8.5 Hz, 1H), 7.60 (dd, *J* = 8.6, 1.9 Hz, 1H), 7.55 (s, 1H), 6.83 (t, *J* = 1.7 Hz, 1H), 6.69 (d, *J* = 1.8 Hz, 2H), 4.15 (t, *J* = 8.6 Hz, 2H), 3.27–3.24 (m, 6H), 3.13–3.10 (m, 4H), 2.26 (s, 3H); HRMS (ESI) *m/z* 454.0753 [(M + H)<sup>+</sup> calcd for C<sub>20</sub>H<sub>21</sub>Cl<sub>2</sub>N<sub>3</sub>O<sub>3</sub>S 454.0759].

5-((4-(3-Chloro-5-(trifluoromethyl)phenyl)piperazin-1-yl)sulfonyl)-1*H*-indole (**16**). To a solution (60 °C) of 1*H*-indole-5-sulfonyl chloride (**15**) (50 mg, 0.23 mmol) and Et<sub>3</sub>N (72 μL, 0.55 mmol) in anhydrous 1,4-dioxane (0.22 M, 1 mL) was added 1-(3-chloro-5-(trifluoromethyl)phenyl)piperazine [**13**] (**14**, 121 mg, 0.46 mmol) in anhydrous 1,4-dioxane (0.5 mL). After stirring at 60 °C for 2 h, the reaction mixture was cooled to 25 °C and stirred for an additional 18 h. The reaction was quenched by an addition of H<sub>2</sub>O and the resulting mixture was diluted with EtOAc. The combined organic layers were washed with brine, dried over anhydrous Na<sub>2</sub>SO<sub>4</sub>, and concentrated *in vacuo*. The residue

was purified by column chromatography (silica gel, hexanes/EtOAc, 3/1) to afford **16** (32 mg, 32%) as a white solid:  $^1\text{H NMR}$  (400 MHz,  $\text{CDCl}_3$ )  $\delta$  8.58 (br s, 1H), 8.15 (s, 1H), 7.60 (d,  $J = 8.5$  Hz, 1H), 7.52 (d,  $J = 8.3$  Hz, 1H), 7.39–7.35 (m, 1H), 7.04 (s, 1H), 6.91 (s, 1H), 6.89 (s, 1H), 6.70 (s, 1H), 3.34–3.26 (m, 4H), 3.20–3.13 (m, 4H); HRMS (ESI)  $m/z$  444.0760  $[(M + H)^+]$  calcd for  $\text{C}_{19}\text{H}_{17}\text{ClF}_3\text{N}_3\text{O}_2\text{S}$  444.0755].

1-(5-((4-(3-Chloro-5-(trifluoromethyl)phenyl)piperazin-1-yl)sulfonyl)-1H-indol-1-yl)ethan-1-one (**17**). To a solution of **16** (15 mg, 0.03 mmol),  $\text{Et}_3\text{N}$  (12  $\mu\text{L}$ , 0.09 mmol), and *N,N*-dimethyl-4-aminopyridine (1.4 mg, 0.012 mmol) in anhydrous 1,2-dichloroethane (1 mL) was added  $\text{Ac}_2\text{O}$  (11.2  $\mu\text{L}$ , 0.12 mmol). The resulting mixture was stirred at 80 °C for 24 h, the reaction was quenched by an addition of  $\text{H}_2\text{O}$ . The mixture was extracted with EtOAc. The combined organic layers were dried over anhydrous  $\text{Na}_2\text{SO}_4$  and concentrated *in vacuo*. The residue was purified by column chromatography (silica gel, hexanes/EtOAc, 3/1) to afford **17** (14 mg, 96%) as a white solid:  $^1\text{H NMR}$  (400 MHz,  $\text{CDCl}_3$ )  $\delta$  8.63 (d,  $J = 8.8$  Hz, 1H), 8.05 (s, 1H), 7.75 (d,  $J = 9.1$  Hz, 1H), 7.58 (d,  $J = 3.7$  Hz, 1H), 7.04 (s, 1H), 6.92 (s, 1H), 6.89 (s, 1H), 6.77 (d,  $J = 3.7$  Hz, 1H), 3.37–3.25 (m, 4H), 3.24–3.12 (m, 4H), 2.69 (s, 3H); HRMS (ESI)  $m/z$  486.0867  $[(M + H)^+]$  calcd for  $\text{C}_{21}\text{H}_{19}\text{ClF}_3\text{N}_3\text{O}_3\text{S}$  486.0872].

5-((4-(3-Chloro-5-(trifluoromethyl)phenyl)piperazin-1-yl)sulfonyl)indoline (**18**). To a cooled (0 °C) solution of **3** [**13**] (89 mg, 0.18 mmol) in EtOH (0.41 mL) was added *c*-HCl (0.2 mL). The resulting mixture was refluxed for 2 h and then ice water was added followed by 35%  $\text{NH}_4\text{OH}$ . The reaction was extracted with EtOAc. The combined organic layers were dried over anhydrous  $\text{Na}_2\text{SO}_4$  and concentrated *in vacuo* to afford **18** (80 mg). Compound **18** was used in the following step without further purification:  $^1\text{H NMR}$  (400 MHz,  $\text{CDCl}_3$ )  $\delta$  7.42 (d,  $J = 6.2$  Hz, 1H), 7.41 (s, 1H), 7.03 (s, 1H), 6.93 (s, 1H), 6.90 (s, 1H), 6.57 (d,  $J = 8.8$  Hz, 1H), 3.68 (t,  $J = 8.4$  Hz, 2H), 3.32–3.25 (m, 4H), 3.15–3.09 (m, 4H), 3.08 (t,  $J = 8.5$  Hz, 2H).

5-((4-(3-Chloro-5-(trifluoromethyl)phenyl)piperazin-1-yl)sulfonyl)-1-(methylsulfonyl)indoline (**19**). To a solution of **18** (36 mg, 0.08 mmol) in pyridine (3.5 mL) was added methanesulfonyl chloride (0.03 mL, 0.39 mmol). The reaction mixture was stirred at 25 °C for 18 h. The reaction was quenched by an addition of saturated  $\text{NH}_4\text{Cl}$  solution and the organic layer was extracted with  $\text{CH}_2\text{Cl}_2$ . The combined organic layers were dried over anhydrous  $\text{Na}_2\text{SO}_4$  and concentrated *in vacuo*. The residue was purified by column chromatography (silica gel, hexanes/EtOAc, 2/1) to afford **19** as a white solid (29 mg, 67% for 2 steps):  $^1\text{H NMR}$  (400 MHz,  $\text{CDCl}_3$ )  $\delta$  7.62 (d,  $J = 8.5$  Hz, 1H), 7.59 (s, 1H), 7.49 (d,  $J = 7.5$  Hz, 1H), 7.06 (s, 1H), 6.94 (s, 1H), 6.91 (s, 1H), 4.08 (t,  $J = 8.6$  Hz, 2H), 3.33–3.27 (m, 4H), 3.23 (t,  $J = 8.6$  Hz, 2H), 3.17–3.12 (m, 4H), 2.95 (s, 3H); HRMS (ESI)  $m/z$  524.0689  $[(M + H)^+]$  calcd for  $\text{C}_{20}\text{H}_{21}\text{ClF}_3\text{N}_3\text{O}_4\text{S}_2$  524.0687].

Methyl 4-(3-(4-((4-(3-(trifluoromethyl)phenyl)piperazin-1-yl)sulfonyl)phenyl)ureido)butanoate (**21**). To a solution of 4-((4-(3-(trifluoromethyl)phenyl)piperazin-1-yl)sulfonyl)aniline [**12**] (**20a**, 103 mg, 0.26 mmol) and CDI (216 mg, 1.33 mmol) in anhydrous THF (1.3 mL) was added DIPEA (0.23 mL, 1.33 mmol). After stirring at 25 °C for 2 h, methyl 4-aminobutanoate (204 mg, 1.33 mmol) was added to the reaction mixture. After stirring at 25 °C for 1.5 h, the reaction mixture was concentrated under reduced pressure. The residue was purified by column chromatography (silica gel, hexanes/EtOAc, 1/1) to afford **21** (100 mg, 71%) as a colorless oil:  $^1\text{H NMR}$  (400 MHz,  $\text{CDCl}_3$ )  $\delta$  7.64 (d,  $J = 8.5$  Hz, 2H), 7.56 (d,  $J = 8.7$  Hz, 2H), 7.37–7.29 (m, 1H), 7.11 (d,  $J = 7.6$  Hz, 1H), 7.06 (s, 1H), 7.01 (d,  $J = 8.6$  Hz, 1H), 5.55 (br s, 1H), 3.68 (s, 3H), 3.34–3.23 (m, 6H), 3.16–3.08 (m, 4H), 2.41 (t,  $J = 6.8$  Hz, 2H), 1.91–1.83 (m, 2H); HRMS (ESI)  $m/z$  529.1726  $[(M + H)^+]$  calcd for  $\text{C}_{23}\text{H}_{27}\text{F}_3\text{N}_4\text{O}_5\text{S}$  529.1727].

4-(3-(4-((4-(3-(Trifluoromethyl)phenyl)piperazin-1-yl)sulfonyl)phenyl)ureido)butanoic acid (**22**). To a solution of **21** (100 mg, 0.18 mmol) in THF/ $\text{H}_2\text{O}$  (2/1, 1.8 mL) was added 1 N LiOH (0.37 mL) at 25 °C. After stirring for 18 h, the reaction was quenched by an addition of 1 N HCl, and the resulting mixture was diluted with  $\text{CH}_2\text{Cl}_2$ .

The layers were separated, and the aqueous layer was extracted with  $\text{CH}_2\text{Cl}_2$ . The combined organic layers were dried over anhydrous  $\text{Na}_2\text{SO}_4$  and concentrated *in vacuo*. The residue was purified by column chromatography (silica gel,  $\text{CH}_2\text{Cl}_2/\text{MeOH}$  (10/1) to 100% MeCN) to afford **22** (90 mg, 97%) as a colorless oil:  $^1\text{H NMR}$  (400 MHz,  $\text{CD}_3\text{OD}$ )  $\delta$  7.68 (d,  $J = 8.8$  Hz, 2H), 7.62 (d,  $J = 8.7$  Hz, 2H), 7.37 (dd,  $J = 7.8$ , 7.9 Hz, 1H), 7.15 (d,  $J = 8.6$  Hz, 1H), 7.14 (s, 1H), 7.08 (d,  $J = 7.6$  Hz, 1H), 3.28–3.22 (m, 6H), 3.14–3.09 (m, 4H), 2.35 (t,  $J = 7.3$  Hz, 2H), 1.84–1.82 (m, 2H); HRMS (ESI)  $m/z$  515.1570  $[(M + H)^+]$  calcd for  $\text{C}_{22}\text{H}_{25}\text{F}_3\text{N}_4\text{O}_5\text{S}$  515.1571].

*N*-((*tert*-Butyldimethylsilyloxy)-4-(3-(4-((4-(3-(trifluoromethyl)phenyl)piperazin-1-yl)sulfonyl)phenyl)ureido)butanamide (**23**). To a solution of **22** (22 mg, 0.04 mmol) in anhydrous THF (2.86 mL) were added ethyl chloroformate (8  $\mu\text{L}$ , 0.08 mmol) and  $\text{Et}_3\text{N}$  (11  $\mu\text{L}$ , 0.08 mmol). After stirring at 25 °C for 1 h,  $\text{NH}_2\text{OTBS}$  (12.5 mg, 0.08 mmol) in anhydrous MeOH (0.66 mL) was added to the reaction mixture. After stirring at 25 °C for 1 h, the reaction mixture was concentrated *in vacuo*. The residue was purified by column chromatography (silica gel,  $\text{CH}_2\text{Cl}_2/\text{MeOH}$ , 50/1 to 10/1) to afford **23** (23 mg, 85%) as a white solid:  $^1\text{H NMR}$  (400 MHz,  $\text{CD}_3\text{OD}$ )  $\delta$  7.68 (d,  $J = 9.3$  Hz, 2H), 7.62 (d,  $J = 9.1$  Hz, 2H), 7.37 (dd,  $J = 7.9$ , 8.0 Hz, 1H), 7.14 (d,  $J = 7.6$  Hz, 1H), 7.13 (s, 1H), 7.08 (d,  $J = 7.7$  Hz, 1H), 6.35–6.30 (m, 1H), 3.32–3.21 (m, 6H), 3.13–3.09 (m, 4H), 2.17 (t,  $J = 7.4$  Hz, 2H), 1.87–1.78 (m, 2H), 0.95 (s, 9H), 0.16 (s, 6H); HRMS (ESI)  $m/z$  644.2542  $[(M + H)^+]$  calcd for  $\text{C}_{28}\text{H}_{40}\text{F}_3\text{N}_5\text{O}_5\text{Si}$  644.2544].

*N*-Hydroxy-4-(3-(4-((4-(3-(trifluoromethyl)phenyl)piperazin-1-yl)sulfonyl)phenyl)ureido)butanamide (**24**). To a cooled (0 °C) solution of **23** (7.7 mg, 0.01 mmol) in anhydrous  $\text{CH}_2\text{Cl}_2$  (1.7 mL) was added dropwise TFA (0.5 mL). After stirring at 25 °C for 25 min, the reaction mixture was concentrated *in vacuo*. The residue was purified by column chromatography (silica gel,  $\text{CH}_2\text{Cl}_2/\text{MeOH}$ , 10/1) to afford **24** as a white solid (7 mg, quantitative):  $^1\text{H NMR}$  (400 MHz,  $\text{CD}_3\text{OD}$ )  $\delta$  7.68 (d,  $J = 8.7$  Hz, 2H), 7.62 (d,  $J = 8.4$  Hz, 2H), 7.38 (dd,  $J = 7.8$ , 7.8 Hz, 1H), 7.16 (d,  $J = 8.1$  Hz, 1H), 7.14 (s, 1H), 7.09 (d,  $J = 7.8$  Hz, 1H), 3.29–3.19 (m, 6H), 3.15–3.07 (m, 4H), 2.15 (t,  $J = 7.5$  Hz, 2H), 1.87–1.78 (m, 2H); HRMS (ESI)  $m/z$  530.1680  $[(M + H)^+]$  calcd for  $\text{C}_{22}\text{H}_{26}\text{F}_3\text{N}_5\text{O}_5\text{S}$  530.1680].

Methyl 5-(3-(4-((4-(3-(trifluoromethyl)phenyl)piperazin-1-yl)sulfonyl)phenyl)ureido)pentanoate (**25a**). To a solution of **20a** (88 mg, 0.23 mmol) and CDI (185 mg, 1.14 mmol) in THF (1.14 mL) was added DIPEA (0.2 mL, 1.14 mmol). After stirring at 25 °C for 2 h, the reaction mixture was treated with methyl 5-aminopentanoate [**15**] (150 mg, 1.14 mmol) and allowed to stir for 1 h. The reaction mixture was concentrated *in vacuo* and the residue was purified by column chromatography (silica gel, hexanes/EtOAc, 1/1) to afford **25a** (75 mg, 60%) as a colorless oil:  $^1\text{H NMR}$  (400 MHz,  $\text{CDCl}_3$ )  $\delta$  7.73 (s, 1H), 7.62 (d,  $J = 8.9$  Hz, 2H), 7.53 (d,  $J = 8.7$  Hz, 2H), 7.33 (dd,  $J = 8.2$ , 8.2 Hz, 1H), 7.10 (d,  $J = 7.7$  Hz, 1H), 7.05 (s, 1H), 7.00 (d,  $J = 8.2$  Hz, 1H), 5.60 (t,  $J = 5.5$  Hz, 1H), 3.64 (s, 3H), 3.27–3.22 (m, 6H), 3.13–3.11 (m, 4H), 2.33 (t,  $J = 7.1$  Hz, 2H), 1.70–1.62 (m, 2H), 1.58–1.51 (m, 2H).

5-(3-(4-((4-(3-(Trifluoromethyl)phenyl)piperazin-1-yl)sulfonyl)phenyl)ureido)pentanoic acid (**26a**). 1 N LiOH (0.25 mL) was added to **25a** (34 mg, 0.063 mmol) in THF/ $\text{H}_2\text{O}$  (2/1, 0.63 mL) at 25 °C. After stirring at 25 °C for 17 h, the reaction mixture was cooled to 0 °C and acidified with 1 N HCl. After an addition of  $\text{H}_2\text{O}$ , the resulting mixture was extracted with  $\text{CH}_2\text{Cl}_2$ . The organic layers were combined, dried over anhydrous  $\text{Na}_2\text{SO}_4$ , and concentrated *in vacuo*. The residue was purified by column chromatography (silica gel,  $\text{CH}_2\text{Cl}_2/\text{MeOH}$ , 10/1) to afford **26a** (18 mg, 54%) as a white solid:  $^1\text{H NMR}$  (400 MHz,  $\text{CD}_3\text{OD}$ )  $\delta$  7.67 (d,  $J = 9.0$  Hz, 2H), 7.62 (d,  $J = 9.0$  Hz, 2H), 7.37 (dd,  $J = 8.3$ , 8.3 Hz, 1H), 7.15 (d,  $J = 7.4$  Hz, 1H), 7.14 (s, 1H), 7.08 (d,  $J = 7.6$  Hz, 1H), 3.29–3.26 (m, 4H), 3.22 (t,  $J = 6.7$  Hz, 2H), 3.11–3.10 (m, 4H), 2.34 (t,  $J = 8.0$  Hz, 2H), 1.70–1.63 (m, 2H), 1.60–1.53 (m, 2H); HRMS (ESI)  $m/z$  529.1733  $[(M + H)^+]$  calcd for  $\text{C}_{23}\text{H}_{27}\text{F}_3\text{N}_4\text{O}_5\text{S}$  529.1727].

*N*-Hydroxy-5-(3-(4-((4-(3-(trifluoromethyl)phenyl)piperazin-1-yl)sulfonyl)phenyl)ureido)pentanamide (**27a**). Ethyl chloroformate

(6.2 mg, 0.057 mmol) and Et<sub>3</sub>N (8  $\mu$ L) were added to a solution of **26a** (15 mg, 0.028 mmol) in THF (2 mL). After stirring for 1 h, the reaction mixture was treated with NH<sub>2</sub>OTBS (8.4 mg, 0.057 mmol) in MeOH (0.44 mL). After an additional 2 h, NH<sub>2</sub>OTBS (8.4 mg, 0.057 mmol) in MeOH (0.44 mL) was added and the resulting mixture was left to stir for additional 2 h. The reaction mixture was concentrated *in vacuo*, dissolved in CH<sub>2</sub>Cl<sub>2</sub> (2 mL), and treated with TFA (0.17 mL). The resulting mixture was stirred at 0 °C for 1 h and then concentrated *in vacuo* to afford **27a** (8.1 mg, 53% for 2 steps) as a solid: <sup>1</sup>H NMR (400 MHz, CD<sub>3</sub>OD)  $\delta$  7.69 (d, *J* = 8.9 Hz, 2H), 7.62 (d, *J* = 8.9 Hz, 2H), 7.39 (dd, *J* = 7.9, 7.9 Hz, 1H), 7.19 (d, *J* = 8.3 Hz, 1H), 7.18 (s, 1H), 7.11 (d, *J* = 7.5 Hz, 1H), 3.32–3.30 (m, 4H), 3.22 (t, *J* = 6.7 Hz, 2H), 3.14–3.11 (m, 4H), 2.14 (t, *J* = 7.3 Hz, 2H), 1.72–1.63 (m, 2H), 1.61–1.50 (m, 2H); HRMS (ESI) *m/z* 544.1840 [(M + H)<sup>+</sup> calcd for C<sub>23</sub>H<sub>28</sub>F<sub>3</sub>N<sub>5</sub>O<sub>5</sub>S 544.1836].

Methyl 5-(3-(4-((4-(3-chloro-5-(trifluoromethyl)phenyl)piperazin-1-yl)sulfonyl)phenyl)ureido)pentanoate (**25b**). To a solution of **20b** (290 mg, 0.69 mmol) and CDI (561 mg, 3.46 mmol) in anhydrous THF (3.45 mL) was added DIPEA (0.6 mL, 3.46 mmol). After stirring at 25 °C for 2 h, the reaction mixture was transferred to methyl 5-aminopentanoate (114 mg, 0.87 mmol). After stirring at 25 °C for 1.5 h, the reaction mixture was concentrated under reduced pressure and the residue was purified by column chromatography (silica gel, hexanes/EtOAc, 1/1) to afford **25b** (350 mg, 87%) as a white sticky solid: <sup>1</sup>H NMR (400 MHz, CDCl<sub>3</sub>)  $\delta$  7.63 (s, 1H), 7.59 (d, *J* = 8.5 Hz, 2H), 7.49 (d, *J* = 8.2 Hz, 2H), 7.05 (s, 1H), 6.95 (s, 1H), 6.93 (s, 1H), 5.56 (br s, 1H), 3.65 (s, 3H), 3.34–3.20 (m, 6H), 3.15–3.06 (m, 4H), 2.33 (t, *J* = 7.2 Hz, 2H), 1.69–1.59 (m, 2H), 1.58–1.50 (m, 2H).

5-(3-(4-((4-(3-Chloro-5-(trifluoromethyl)phenyl)piperazin-1-yl)sulfonyl)phenyl)ureido)pentanoic acid (**26b**). To a solution of **25b** (34 mg, 0.05 mmol) in THF/H<sub>2</sub>O (2/1, 0.5 mL) was added 1 N LiOH (0.13 mL) at 25 °C. After stirring for 18 h, the reaction was quenched by an addition of 1 N HCl, and the resulting mixture was diluted with CH<sub>2</sub>Cl<sub>2</sub>. The layers were separated, and the aqueous layer was extracted with CH<sub>2</sub>Cl<sub>2</sub>. The combined organic layers were dried over anhydrous Na<sub>2</sub>SO<sub>4</sub> and concentrated *in vacuo*. The residue was purified by column chromatography (silica gel, CH<sub>2</sub>Cl<sub>2</sub>/MeOH (30/1) to 100% MeCN) to afford **26b** (15 mg, 45%) as a white solid: <sup>1</sup>H NMR (400 MHz, CD<sub>3</sub>COCD<sub>3</sub>)  $\delta$  8.60 (s, 1H), 7.75 (d, *J* = 8.6 Hz, 2H), 7.65 (d, *J* = 8.6 Hz, 2H), 7.20 (s, 1H), 7.17 (s, 1H), 7.06 (s, 1H), 6.18 (br s, 1H), 3.50–3.41 (m, 4H), 3.27–3.24 (m, 2H), 3.15–3.07 (m, 4H), 2.33 (t, *J* = 7.2 Hz, 2H), 1.67–1.64 (m, 2H), 1.59–1.56 (m, 2H); HRMS (ESI) *m/z* 563.1340 [(M + H)<sup>+</sup> calcd for C<sub>23</sub>H<sub>26</sub>ClF<sub>3</sub>N<sub>4</sub>O<sub>5</sub>S 563.1337].

*N*-Hydroxy-5-(3-(4-((4-(3-chloro-5-(trifluoromethyl)phenyl)piperazin-1-yl)sulfonyl)phenyl)ureido)-pentanamide (**27b**). [Coupling Reaction] To a solution of **26b** (13 mg, 0.02 mmol) in anhydrous THF (1.69 mL) were added ethyl chloroformate (4.3  $\mu$ L, 0.04 mmol) and Et<sub>3</sub>N (6  $\mu$ L, 0.04 mmol). After stirring at 25 °C for 1 h, NH<sub>2</sub>OTBS (6 mg, 0.04 mmol) in anhydrous MeOH (0.39 mL) was added to the reaction mixture. After stirring at 25 °C for 1 h, the reaction mixture was concentrated *in vacuo* and purified by column chromatography (silica gel, CH<sub>2</sub>Cl<sub>2</sub>/MeOH, 30/1) to afford *N*-((*tert*-butyldimethylsilyloxy)-5-(3-(4-((4-(3-chloro-5-(trifluoromethyl)phenyl)piperazin-1-yl)sulfonyl)phenyl)ureido)pentanamide (13 mg) as a white solid: <sup>1</sup>H NMR (400 MHz, CD<sub>3</sub>COCD<sub>3</sub>)  $\delta$  9.78 (br s, 1H), 8.46 (s, 1H), 7.74 (d, *J* = 9.2 Hz, 2H), 7.66 (d, *J* = 8.9 Hz, 2H), 7.20 (s, 1H), 7.17 (s, 1H), 7.06 (s, 1H), 6.04 (t, *J* = 5.5 Hz, 1H), 3.50–3.42 (m, 4H), 3.26–3.19 (m, 2H), 3.15–3.07 (m, 4H), 2.15–2.13 (m, 2H), 1.69–1.60 (m, 2H), 1.56–1.53 (m, 2H), 0.94 (s, 9H), 0.15 (s, 6H); HRMS (ESI) *m/z* 692.2313 [(M + H)<sup>+</sup> calcd for C<sub>29</sub>H<sub>41</sub>ClF<sub>3</sub>N<sub>5</sub>O<sub>5</sub>SSi 692.2311]; [TBS Deprotection] To a cooled (0 °C) solution of the TBS protected hydroxamic acid (13 mg, 0.01 mmol) in anhydrous CH<sub>2</sub>Cl<sub>2</sub> (2.8 mL) was added dropwise TFA (240  $\mu$ L). After stirring for 25 min at 25 °C, the reaction mixture was concentrated *in vacuo* and purified by column chromatography (silica gel, CH<sub>2</sub>Cl<sub>2</sub>/MeOH, 10/1) to afford **27b** (7 mg, 55% for 2 steps) as a white solid: <sup>1</sup>H NMR (400 MHz, CD<sub>3</sub>COCD<sub>3</sub>)  $\delta$

10.04 (br s, 1H), 8.09 (br s, 1H), 7.74 (br s, 2H), 7.66 (br s, 2H), 7.21 (s, 1H), 7.18 (s, 1H), 7.06 (s, 1H), 3.49–3.37 (m, 4H), 3.26–3.18 (m, 2H), 3.12–3.10 (m, 4H), 2.19–2.11 (m, 2H), 1.70–1.59 (m, 2H), 1.56–1.48 (m, 2H); HRMS (ESI) *m/z* 578.1441 [(M + H)<sup>+</sup> calcd for C<sub>23</sub>H<sub>27</sub>ClF<sub>3</sub>N<sub>5</sub>O<sub>5</sub>S 578.1446].

#### 4.2. Cloning and purification of *K. Pneumoniae* LpxH

Cloning and purification of *K. pneumoniae* LpxH for crystallography studies were carried out as previously reported [13]. Briefly, *K. pneumoniae* LpxH was cloned into a modified pET21b (Novagen/Millipore Sigma) vector, yielding the LpxH fusion protein with a C-terminal TEV protease site (ENLYFQGS) and His<sub>10</sub> tag. Vector-transformed BL21 STAR (DE3) *E. coli* cells (Thermo Fisher Scientific) were grown in M9 minimal medium to an OD<sub>600</sub> of 0.5 at 37 °C, prior to being induced with 1 mM IPTG at 30 °C. After 5 h, the cells were then harvested by centrifugation. Protein purification was carried out at 4 °C. Cell pellets were lysed in a buffer containing 50 mM phosphate-citrate, 20 mM MES (pH 6.0), 600 mM NaCl, 10% sucrose, 5 mM 2-mercaptoethanol, 10 mM imidazole, and 0.1% Triton X-100 using a French press. After removing cell debris by centrifugation, a HisPur Ni-NTA column (Thermo Fisher Scientific) was pre-equilibrated with the lysis buffer, and the supernatant was loaded. Following extensive washes using a purification buffer containing 20 mM phosphate-citrate, 20 mM MES (pH 6.0), 300 mM NaCl, 5% glycerol, 5 mM 2-mercaptoethanol, and 40 mM imidazole, LpxH was eluted from the column by increasing the imidazole concentration stepwise from 40 to 400 mM. The protein sample was concentrated and further purified with size-exclusion chromatography (Superdex 200; GE Healthcare Life Sciences) in the FPLC buffer containing 20 mM MES (pH 6.0), 800 mM NaCl, 1 mM DTT, and 5% glycerol.

#### 4.3. Co-crystallization of *K. Pneumoniae* LpxH with a sulfonyl piperazine antibiotic **27b** (JH-LPH-41)

Peak fractions containing *K. pneumoniae* LpxH were buffer-exchanged into a buffer containing 20 mM MES (pH 6.0), 200 mM NaCl, 1 mM DTT, and 5% glycerol. During buffer exchange, concentrated **27b** solution in DMSO was added to the protein solution in a 1:1 M ratio. The solution was then concentrated to 8 mg/mL for crystallization and additional concentrated **27b** solution in DMSO was added to the protein solution in a 1:1 M ratio (final ratio = 2:1 drug: protein, final **27b** concentration = 0.54 mM, DMSO = 2%).

Protein crystals were grown using the sitting-drop vapor diffusion method at 20 °C. Each drop was prepared by mixing 1  $\mu$ L of the protein solution with 1  $\mu$ L of the reservoir solution (200 mM KCl, 100 mM sodium citrate, 37% pentaerythritol propoxylate (5/4 PO/OH), pH 5.5). The final drop solution contained 4 mg/mL of LpxH with 0.27 mM **27b**, 10 mM MES (pH 6.0), 100 mM NaCl, 100 mM KCl, 50 mM sodium citrate (pH 5.5), 18.5% pentaerythritol propoxylate (5/4 PO/OH), 0.5 mM DTT, 1% DMSO, and 2.5% glycerol. Diffraction quality protein crystals were harvested after 2 weeks and soaked with the reservoir solution additionally containing 20% glycerol, 100  $\mu$ M MnCl<sub>2</sub>, 0.27 mM **27b**, and 2% DMSO for cryoprotection.

#### 4.4. Structural analysis of *K. Pneumoniae* LpxH complexes with **27b** (JH-LPH-41)

The X-ray diffraction data of the *K. pneumoniae* LpxH complex with **27b** were collected at the Northeastern Collaborative Access Team (NECAT) 24-ID-C beamline at the Advanced Photon Source at Argonne National Laboratory. The X-ray diffraction data was processed using XDS [16]. The phase information of the crystal structures of the *K. pneumoniae* LpxH complex was obtained by molecular replacement with the PHASER module in the PHENIX suite [17] using the PDB entry 6PJ3 as the search model. Restraints of the inhibitors were generated by

using eLBOW [18] and edited manually. Iterative model building and refinement was carried out using COOT [19] and PHENIX [17]. The 2mFo-DFc omit maps were generated using PHENIX [17].

#### 4.5. Enzymatic assay for LpxH inhibition

The LpxE-coupled LpxH activity assay [12] was conducted as described previously using the GB1-*K. pneumoniae* LpxH-His<sub>10</sub> fusion protein [13]. Briefly, two reaction mixtures were prepared that contain 20 mM Tris-HCl (pH 8.0), 0.5 mg/mL BSA, 0.02% Triton X-100, 1 mM MnCl<sub>2</sub>, 1 mM DTT, and 10% DMSO, with one additionally containing 200 μM substrate (UDP-DAGn) and the other containing both LpxH (20 ng/mL) and 0.2 μM inhibitor. The reaction mixtures were pre-incubated at 37 °C for 10 min before an equal volume of the LpxH mixture was added to the substrate mixture to initiate the reaction at 37 °C. The final reaction solution contains 100 μM substrate, 10 ng/mL enzyme, and 0.1 μM inhibitor. At the desired reaction time points, an aliquot of 20 μL reaction mixture was removed and added to a well in 96-well half-area plate containing 5 mM EDTA (final concentration) to quench the LpxH reaction. Purified *Aquifex aeolicus* LpxE was then added to a final concentration of 5 μg/mL. The plate was incubated at 37 °C for 30 min followed by addition of formic acid to a final concentration of 3.75 M to quench the LpxE reaction. The malachite green reagent (Sigma Aldrich, catalog MAK307) was added with a 5-fold dilution, and the solution was incubated for 30 min at room temperature before the absorbance at 620 nm was measured. All measurements were done in triplicates, and standard error was calculated. Percentage LpxH activities for 1, 2, and 3 at 0.1 μM were calculated from previously reported IC<sub>50</sub> values [13], which were extracted from fitting of the dose-response curve of  $v_i/v_0 = 1/(1 + [I]/IC_{50})$  assayed under identical conditions.

#### Author contributions

S.-H.K. and C.S.C. contributed equally; P.Z. and J.H. conceived the project, designed the overall experimental strategy, and analyzed and discussed the results; S.-H.K., A.F.E., W.Y.L., and C.G.W. synthesized the sulfonyl piperazine LpxH inhibitors used in this study; C.S.C. purified lipid X and UDP-DAGn, and characterized the inhibitory effect of LpxH inhibitors; C.S.C. and J.C. purified and crystallized the *K. pneumoniae* LpxH/27b complex; C.S.C., B.A.F., and P.Z. determined the crystal structure; P.Z. and J.H. wrote the manuscript with input from all the authors and held overall responsibility for the study.

#### Declaration of Competing Interest

The authors declared that there is no conflict of interest.

#### Acknowledgments

This work was supported in part by the grants from the National Institute of Allergy and Infectious Diseases (AI139216) and National Institute of General Medical Sciences (GM115355). X-ray diffraction data were collected at the Northeastern Collaborative Access Team beam lines (24-ID-C), which is funded by the National Institute of General Medical Sciences from the National Institutes of Health (P30 GM124165). The Pilatus 6 M detector on 24-ID-C beam line is funded by a NIH-ORIP HEI grant (S10 RR029205). This research used resources of the Advanced Photon Source, Department of Energy Office of Science, United States User Facility operated for the Department of Energy Office of Science by Argonne National Laboratory under Contract No. DE-AC02-06CH11357. C.G.W. and A.F.E. were supported by the NIGMS Pharmacological Sciences Training Grant (NIH

GM007105). The authors would like to thank Dr. Jinshi Zhao for insightful discussions about the LpxH inhibition assay.

#### Appendix A. Supplementary material

Supplementary data to this article can be found online at <https://doi.org/10.1016/j.bioorg.2020.104055>.

#### References

- [1] H.W. Boucher, G.H. Talbot, J.S. Bradley, J.E. Edwards, D. Gilbert, L.B. Rice, M. Scheld, B. Spellberg, J. Bartlett, Bad bugs, no drugs: no ESKAPE! An update from the infectious diseases society of America, *Clin. Infect. Dis.* 48 (1) (2009) 1–12, <https://doi.org/10.1086/595011>.
- [2] WHO Global priority list of antibiotic-resistant bacteria to guide research, discovery, and development of new antibiotics; World Health Organization, 2017.
- [3] C.R.H. Raetz, C. Whitfield, Lipopolysaccharide endotoxins, *Annu. Rev. Biochem.* 71 (2002) 635–700, <https://doi.org/10.1146/annurev.biochem.71.110601.135414>.
- [4] A.W. Barb, P. Zhou, Mechanism and inhibition of LpxC: an essential zinc-dependent deacetylase of bacterial lipid A synthesis, *Curr. Pharm. Biotechnol.* 9 (1) (2008) 9–15, <https://doi.org/10.2174/138920108783497668>.
- [5] P. Zhou, J. Zhao, Structure, inhibition, and regulation of essential lipid A enzymes, *Biochim. Biophys. Acta (BBA) – Molecular Cell Biol. Lipids* 1862 (11) (2017) 1424–1438, <https://doi.org/10.1016/j.bbalip.2016.11.014>.
- [6] K.J. Babinski, A.A. Ribeiro, C.R.H. Raetz, The *Escherichia coli* gene encoding the UDP-2,3-diacetylglucosamine pyrophosphatase of lipid A biosynthesis, *J. Biol. Chem.* 277 (29) (2002) 25937–25946, <https://doi.org/10.1074/jbc.M204067200>.
- [7] L.E. Metzger IV, C.R.H. Raetz, An alternative route for UDP-diacetylglucosamine hydrolysis in bacterial lipid A biosynthesis, *Biochemistry* 49 (31) (2010) 6715–6726, <https://doi.org/10.1021/bi1008744>.
- [8] H.E. Young, J. Zhao, J.R. Barker, Z. Guan, R.H. Valdivia, P. Zhou, Discovery of the elusive UDP-diacetylglucosamine hydrolase in the lipid A biosynthetic pathway in *Chlamydia trachomatis*, *mBio* 7 (2) (2016) e00090–16, <https://doi.org/10.1128/mBio.00090-16>.
- [9] L.E. Metzger IV, J.K. Lee, J.S. Finer-Moore, C.R.H. Raetz, R.M. Stroud, LpxI structures reveal how a lipid A precursor is synthesized, *Nat. Struct. Mol. Biol.* 19 (11) (2012) 1132–1138, <https://doi.org/10.1038/nsmb.2393>.
- [10] L.E. Metzger IV, C.R.H. Raetz, Purification and characterization of the lipid A disaccharide synthase (LpxB) from *Escherichia coli*, a peripheral membrane protein, *Biochemistry* 48 (48) (2009) 11559–11571, <https://doi.org/10.1021/bi901750f>.
- [11] A.S. Nayar, T.J. Dougherty, K.E. Ferguson, B.A. Granger, L. McWilliams, C. Stacey, L.J. Leach, S. Narita, H. Tokuda, A.A. Miller, D.G. Brown, S.M. McLeod, Novel antibacterial targets and compounds revealed by a high-throughput cell wall reporter assay, *J. Bacteriol.* 197 (10) (2015) 1726–1734, <https://doi.org/10.1128/JB.02552-14>.
- [12] M. Lee, J. Zhao, S.H. Kwak, J. Cho, M. Lee, R.A. Gillespie, D.Y. Kwon, H. Lee, H.J. Park, Q. Wu, P. Zhou, J. Hong, Structure-activity relationship of sulfonyl piperazine LpxH inhibitors analyzed by an LpxE-coupled malachite green assay, *ACS Infect. Dis.* 5 (4) (2019) 641–651, <https://doi.org/10.1021/acsinfecdis.8b00364>.
- [13] J. Cho, M. Lee, C.S. Cochrane, C.G. Webster, B.A. Fenton, J. Zhao, J. Hong, P. Zhou, Structural basis of the UDP-diacetylglucosamine pyrophosphohydrolase LpxH inhibition by sulfonyl piperazine antibiotics, *Proc. Natl. Acad. Sci. USA* 117 (8) (2020) 4109–4116, <https://doi.org/10.1073/pnas.1912876117>.
- [14] F. Huguet, A. Melet, R. Alves de Sousa, A. Lieutaud, J. Chevalier, L. Maigre, P. Deschamps, A. Tomas, N. Leulliot, J.M. Pages, I. Artaud, Hydroxamic acids as potent inhibitors of Fe(II) and Mn(II) *E. coli* methionine aminopeptidase: biological activities and X-ray structures of oxazole hydroxamate-EcMetAP-Mn complexes, *ChemMedChem* 7 (6) (2012) 1020–1030, <https://doi.org/10.1002/cmdc.201200076>.
- [15] L. Gros, S.O. Lorente, C.J. Jimenez, V. Yardley, L. Rattray, H. Wharton, S. Little, S.L. Croft, L.M. Ruiz-Perez, D. Gonzalez-Pacanowska, I.H. Gilbert, Evaluation of azasterols as anti-parasitics, *J. Med. Chem.* 49 (20) (2006) 6094–6103, <https://doi.org/10.1021/jm060290f>.
- [16] W. Kabsch, *Xds Acta Crystallographica Section D, Biol. Crystallogr.* 66 (2) (2010) 125–132, <https://doi.org/10.1107/S0907444909047337>.
- [17] P.D. Adams, P.V. Afonine, G. Bunkoczi, V.B. Chen, I.W. Davis, N. Echols, J.J. Headd, L.W. Hung, G.J. Kapral, R.W. Grosse-Kunstleve, A.J. McCoy, N.W. Moriarty, R. Oeffner, R.J. Read, D.C. Richardson, J.S. Richardson, T.C. Terwilliger, P.H. Zwart, PHENIX: a comprehensive Python-based system for macromolecular structure solution, *Acta Crystallogr. D Biol. Crystallogr.* 66 (2) (2010) 213–221, <https://doi.org/10.1107/S0907444909052925>.
- [18] N.W. Moriarty, R.W. Grosse-Kunstleve, P.D. Adams, electronic Ligand Builder and Optimization Workbench (eLBOW): a tool for ligand coordinate and restraint generation, *Acta Crystallogr. D Biol. Crystallogr.* 65 (10) (2009) 1074–1080, <https://doi.org/10.1107/S0907444909029436>.
- [19] P. Emsley, K. Cowtan, Coot: model-building tools for molecular graphics, *Acta Crystallogr. D Biol. Crystallogr.* 60 (12) (2004) 2126–2132, <https://doi.org/10.1107/S0907444904019158>.